Iranian Journal of Oil & Gas Science and Technology, Vol. 4 (2015), No. 1, pp. 17-34
http://ijogst.put.ac.ir

Organic Geochemistry and Paleoenvironments of Deposition of the Middle Jurassic Sediments from the Tabas Basin, Central Iran

Bahram Alizadeh[1], Majid Alipour[1*], Bahram Habibnia[2], Ahmad Reza Gandomi-Sani[3], Behzad Khani[4], Saber Shirvani[1], and Amir Abbas Jahangard[1]

[1] Department of Geology, Faculty of Earth Sciences, Shahid Chamran University, Ahwaz, Iran
[2] Department of Exploration Engineering, Petroleum University of Technology, Abadan, Iran
[3] National Iranian Oil Company (Exploration Directorate), Tehran, Iran
[4] Department of Geology, Research Institute of Petroleum Industry (RIPI), Tehran, Iran

Received: June 04, 2014*; revised*: September 29, 2014*; accepted*: October 15, 2014

Abstract

In an attempt to reconstruct the paleoenvironments of deposition for the Middle Jurassic Baghamshah formation, samples collected from six outcrop sections along the Shotori swell were subjected to detailed geochemical analyses. Bulk geochemical and biological marker data indicate a logical trend of the variation of organic input, salinity, and oxicity within Baghamshah paleoenvironments across the studied area. An increase in terrestrial character from southern end towards the central parts of the Shotori swell parallels with a uniform increase in the oxicity and a decrease in the salinity. The northernmost sections are characterized by less terrestrial impact, reduced oxicity, and elevated salinity compared to the central and southern sections. These variations are interpreted in the framework of past geometric configuration and a hypothetical paleogeomorphologic model is tentatively proposed for the Middle Jurassic of the area. According to these results, the depositional setting of the studied formation decreased in depth from Section-1 towards Section-4, suggesting that the proximity of the latter section to the Yazd Block may have had a strong control over the observed geochemical variations. The terrestrial organic input and the oxicity of the environment are conspicuously low for northern sections and their salinity shows a sharp increase compared to other sections. We hypothesize that a fault plan exists across the northern and southern Shotori Mountains that had played an active role in creating the current geochemical variations.

Keywords: Paleoreconstruction, Biological Markers, Middle Jurassic, Tabas Basin, Central Iran

1. Introduction

Organic geochemical data from outcrop samples require careful handling with knowledge of the geological history of the area and the occurrence and extent of various surface processes that may disguise maturity, facies, and paleoenvironmental imprints. The effects of weathering on both molecular and bulk geochemical properties of organic matter (OM) have been studied (Clayton and King, 1987; Leythaeuser, 1973; Lo and Cardott, 1995; Marynowski et al., 2011). Likewise, inferring about the past depositional conditions of hydrocarbon source layers has become increasingly commonplace (Alizadeh et al., 2011; Mello et al., 1988; Ortiz et al., 2013; Rodrigues et al., 1988; Seifert and Moldowan, 1981; Ten Haven et al., 1988).

This study undertakes a multifaceted analytical scheme in order to assess the geochemical

* Corresponding Author:
Email: alipour.magid@gmail.com

characteristics of Middle Jurassic Baghamshah formation based on the samples taken from 6 outcrop sections along the Shotori Mountains (Figure 1). The combined application of organic geochemical parameters has been shown by numerous studies to draw reliable inferences about the past depositional conditions of hydrocarbon source rocks. Sedimentary organic matter holds a wealth of geochemical information that can be used for such reconstructions. As an organic geochemical study, this paper reports on some organic geochemical data to infer about the paleodepositional conditions; yet hope remains that other studies (such as stratigraphy and sedimentary geochemistry) will also consider investigation of the past conditions for these sediments by using their own methodologies.

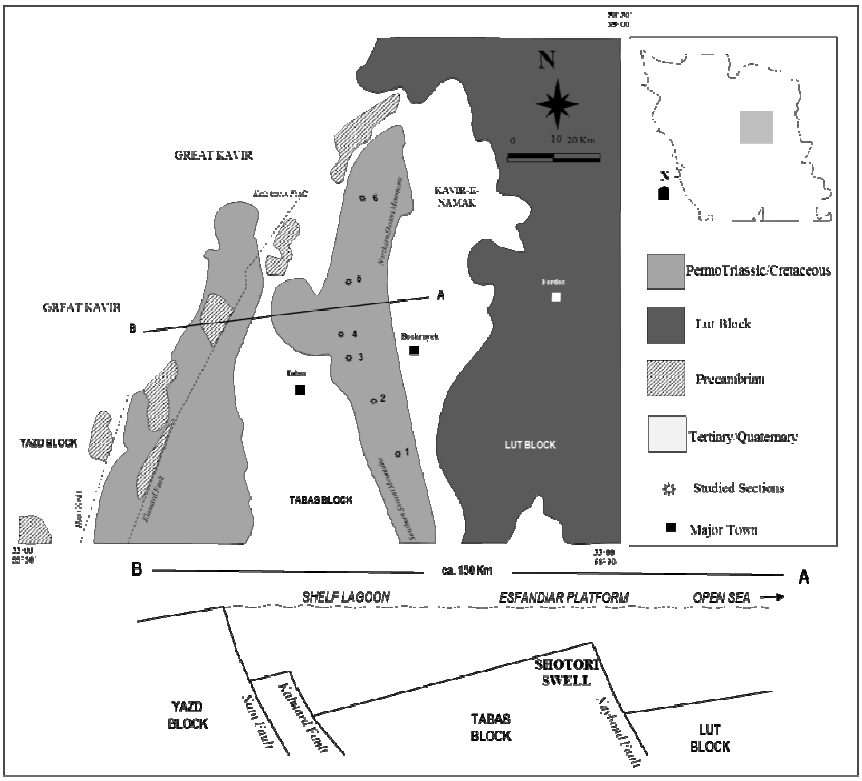

Figure 1

Major structural blocks in Central Iran; the east-west cross section (line A-B) represents the Middle-Upper Jurassic (Callovian-Oxfordian) configuration of the area (after Wilmsen et al., 2009).

It is worth mentioning that one sample from each of these sections is selected for detailed analyses except for sections 3, 5, and 6, where two samples were selected from the lower and upper parts of the Baghamshah formation respectively (Figure 3 and Table 2). Therefore, a total of 9 samples out of 121 samples were selected for the complementary analyses as shown in Figure 3 and also listed in Table 2. The purpose of the current study is to deduce the paleoenvironments in which the studied formation was deposited based on bulk and molecular geochemical properties of extractable OM. The Middle Jurassic marls investigated here show a uniform and relatively high level of thermal maturity in all the studied sections (mid-late oil window as suggested by the average T_{max} value of 460 °C, average *Ro* of 0.72% in Table 1, and sterane and terpane maturity indices in Table 2); a fact that allows us to relate differences in various parameters among sections to factors other than maturity (OM type and depositional conditions). Moreover, it is suggested that surface weathering processes have not drastically altered the various geochemical parameters we use in our interpretations.

Table 1
Average vitrinite reflectance and bulk geochemical data for the Baghamshah samples within the studied sections.

Section	Ro (%)			T_{max} (°C)			TOC (wt.%)			HI (mg HC/g TOC)			OI (mg HC/g TOC)		
	Ave	Min	Max	Ave	Min	Max	Ave	Min	Max	Ave	Min	Max	Ave	Min	Max
Section-1	0.74	0.68	0.78	481	414	608	0.43	0.25	0.62	27.5	4.0	84.2	146	74	208
Section-2	0.67	0.65	0.70	444	401	498	0.35	0.23	0.46	61.5	36.9	91.3	201	124	397
Section-3	0.70	0.53	0.90	468	424	516	0.34	0.13	0.46	10.8	4.35	15.3	240	114	462
Section-4	0.60	0.58	0.65	438	384	497	0.35	0.27	0.50	24.9	3.0	85	266	105	836
Section-5	0.88	0.69	1.0	476	318	604	0.60	0.18	0.98	7.80	1.0	23	71.6	32	272
Section-6	0.95	0.90	1.0	488	397	609	0.40	0.29	0.75	33.2	9.0	53	82.5	15	120

In a previous study, Alizadeh et al. (2011) studied the paleoenvironments in the same area for Upper Triassic–Middle Jurassic sediments (including Nayband and Ab-e-Haji formations); in the present study, however, our focus is on the Baghamshah formation (Mid-Jurassic) and its paleoenvironments. Although the analytical procedure is the same, the scope of the two papers is entirely different. Alizadeh et al. (2011) studied the vertical variations in sedimentary conditions through geologic time at one single location (namely the Kamarmacheh Kuh section), while this papers reconstructs the past conditions within a specific period of geologic time (Baghamshah formation deposition) throughout the entire Shotori region. In a more strict sense, the results from the previous study are more of a scientific significance (how the depositional conditions change by passing from Triassic to Jurassic at that particular location), while the present paper provides some evidence on the past geometry of the area in a regional sense during deposition of Baghamshah formation.

2. Geological setting and structural history

The Shotori swell has been known to exist as a positive geological feature throughout most of the Jurassic time, beginning to rise since the Late Triassic time (Fürsich et al., 2003; Stöcklin et al., 1965). A detailed account of the structural evolution of this swell throughout the Callovian stage is provided by Fürsich et al. (2003). The authors use the sedimentary record of the area to explain the evolving configuration of this west-vergent fault-block (Fürsich et al., 2003; Wilmsen et al., 2010). A renewal of the uplifting movements in the Early Callovian resulted in the extensive erosion of the underlying Baghamshah formation to form the synsedimentary Sikhur formation, and the subsequent formation of an extensive carbonate platform (the Esfandiar platform) (Seyed-Emami et al., 2004; Wilmsen et al., 2009; Wilmsen et al., 2010). Over the steep flank of this platform (towards the east), deep-water sediments of the Qal'eh-Dokhtar formation were formed, while in the west, the shelf-lagoonal deposits of Kamar-e-Mehdi formation were deposited (Fürsich et al., 2003; Seyed-Emami et al., 2004; Wilmsen et al., 2009) (cross section in Figure 1).

3. Stratigraphy

Generally, the Mesozoic within the central Iran is referred to as post-orogenic strata deposited following the collision of the Iranian plate with Eurasia and having registered tectonic events of varying magnitude and areal extent (Fürsich et al., 2003). Seyed-Emami et al. (2004) provides a detailed description of these events during the Mid-Late Jurassic time. Moreover, the Jurassic stratigraphy of the central Iran in relation to these structural events is described in detail (Wilmsen et al., 2009; Wilmsen et al., 2010).

4. Methodology

A total of 121 samples were collected from 6 outcrop sections under a systematic sampling scheme (Figure 1). Special care was taken in sample collection as to minimize the effects of surface alteration (at least 50 cm below the surface). These samples were subjected to Rock-Eval 6 pyrolysis following the method described in the literature (Espitalié et al., 1977). 50-100 mg aliquots of ground samples were heated at 300 °C for 3 minutes and then the temperature increased at a rate of 25 °C/min up to 550 °C under a constant flow of inert gas. The pyrolysis products were swept into a flame ionization detector and were recorded as basic geochemical parameters (TOC, S_1, S_2, and S_3). Samples with favorable quality were selected for further complementary analyses. Noting that all the samples in our study come from outcrop sections, two main screening criteria were applied to our dataset: (1) the level of organic richness (represented by the TOC) and (2) their color in the hand specimen. In each of the sections, it was desired to select samples with the highest TOC values and the darkest color for further analyses. The soluble part of the associated organic matter was extracted using a soxhlet extractor, deasphaltened and further sub-fractionated into saturate, aromatic, and NSO components by using alumina and silica columns. Subsequently, the saturate subfraction was analyzed by a Hewlett Packard 5890 gas chromatogram equipped with a flame ionization detector (FID) and fitted with a 25-m fused silica capillary column. A similar GC device coupled with a VG 7250 mass spectrometer was employed for the GCMS analysis of both the saturate and the aromatic fractions in the SIM mode.

5. Results and discussion

The geochemical parameters of interest obtained from the GC and GCMS analyses of the extractable OM are listed in Table 2 for the studied sections. It is worth mentioning that, according to the Rock-Eval pyrolysis results (HI vs. OI diagrams in Figure 2b and Table 1), most of the analyzed samples are categorized as bearing type IV kerogen by occupying a position near the horizontal axis. However, accurate judgment about the nature of the OM relies on the knowledge of organic contents (Dembicki Jr, 2009) and matrix effects (Katz, 1983). In the following, the geochemical properties of each of the sections are reported in detail.

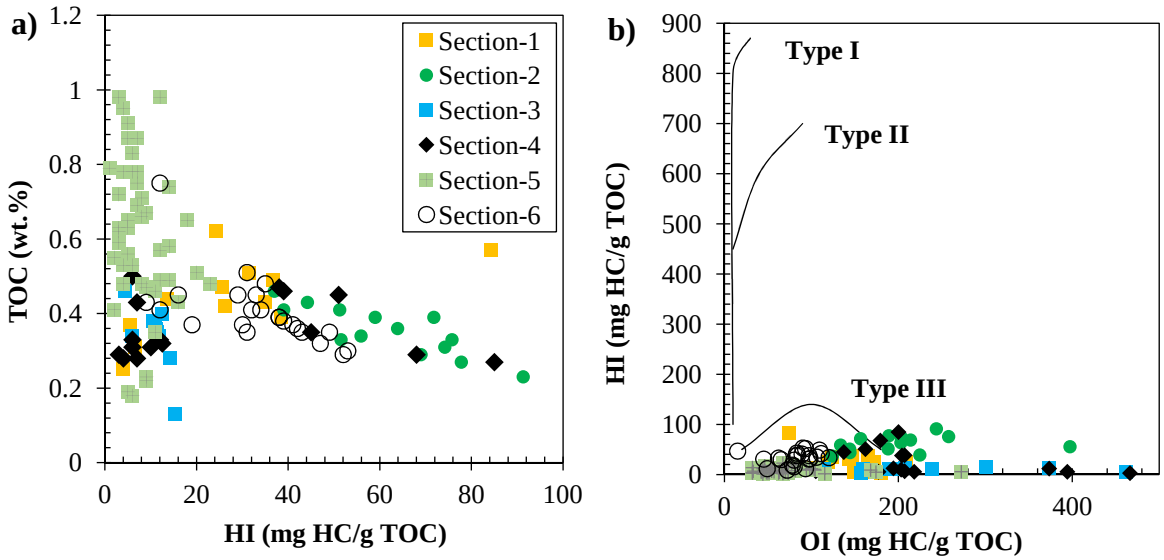

Figure 2
Variations of TOC and HI values for the samples from six studied sections (a) and the HI versus OI diagram for determining the quality of the organic matter (b).

5.1. Section 1

The Baghamshah formation in this section comprises of around 550 m of homogenous marls with green to gray/dark gray color in the outcrop (Figure 3). For the samples from this section, samples with higher TOC readings are associated with higher HI values (Figure 2a) and there is a decrease in the OI with increasing TOC. The gas chromatographic profile for a sample from Section 1 (Figure 4) indicates a predominance of n-alkanes in the C_{15}-C_{16} range with a rather slight even-to-odd preference, typical of OM deposited in marine environments (Hunt, 1996; Peters et al., 2005). The relatively low concentrations of isoprenoids over the GC profile of this sample may denote a lower contribution from photosynthetic plants (Goossens et al., 1984). In addition, the overall absence of the higher molecular weight (HMW) n-alkanes and the low TAR ratio (0.18) are clues that suggest small terrestrial contribution in this locality (Peters et al., 2005).

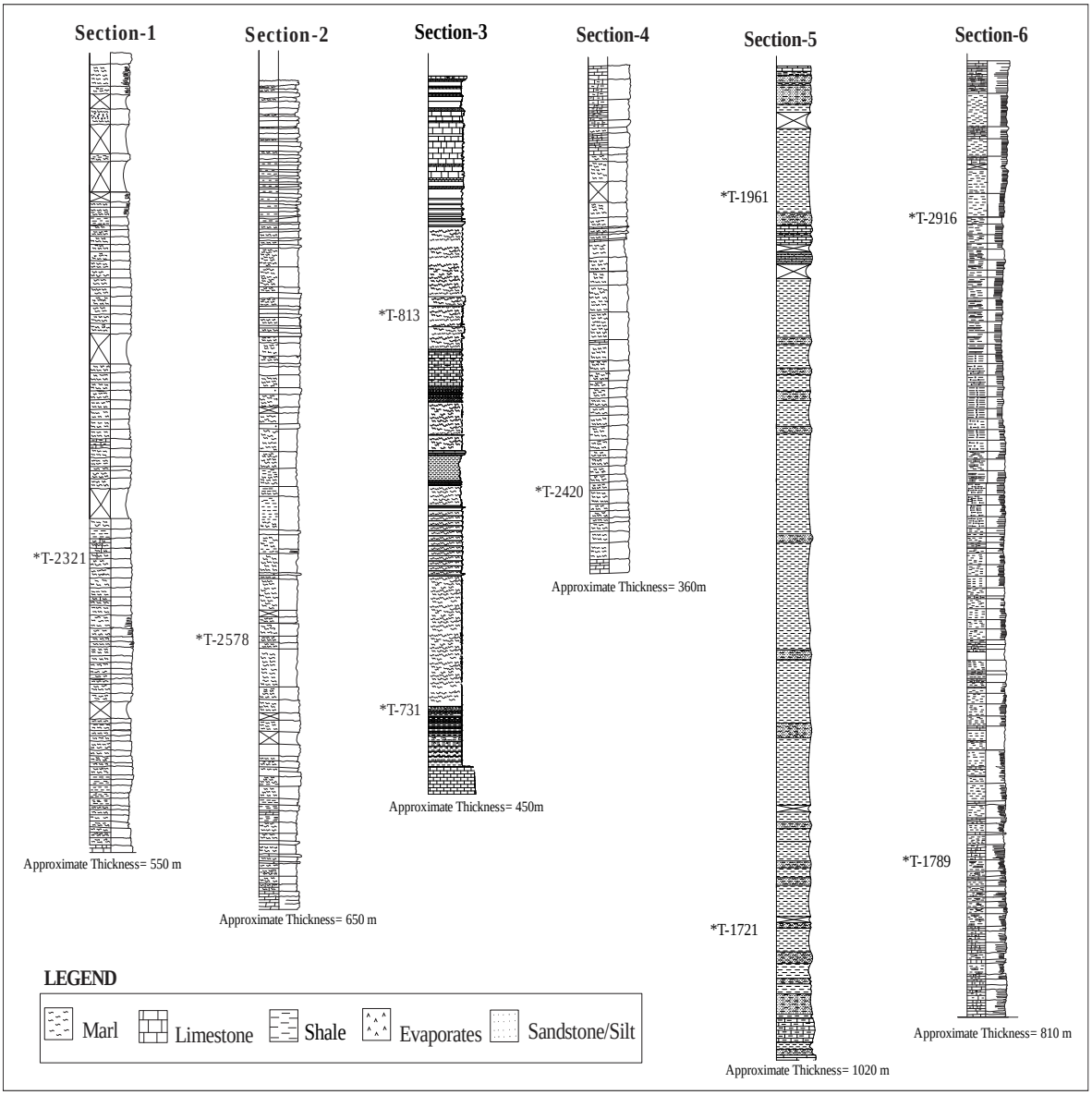

Figure 3
A generalized illustration of the lithologic properties of the Baghamshah formation among the studied sections; the samples selected for GC and GC-MS analyses are indicated by an asterisk.

The lower terrestrial input in this section is also deduced based on the biological marker data (Table 2) such as the very low $C2_9/C_{27}$ ααα regular sterane ratio (0.58), the very low moretane/hopane ratio (0.12) (Isaksen and Bohacs, 1995), relatively high ratios of C_{29}/C_{30} hopane (0.95) (Zumberge, 1984), and comparatively low value of hopane/sterane ratio (Table 2).

The very low values for Gammacerane Index (GI= 0.11) and the lower concentrations of tricyclic terpanes (Huang, 2000) are indications of the lower salinity of the depositional setting. However, the relatively high value (1.23) for the R_{22} ratio (Ten Haven et al., 1988) and the relatively high DBT/Phen ratio for this section suggest higher salinity conditions in the environment (Table 2). This could be a consequence of the intermittent periods of highly saline and marginally saline conditions in this locality, which have led to an intermediate salinity imprint (i.e. R_{22} value is <1.5).

Several biomarker ratios indicate that the environment of deposition was relatively oxic in this section. The comparatively high (0.34) ratio of the short/(short+long) MAS (Moldowan et al., 1986) together with a relatively low (0.76) value of the C_{35}/C_{34} homohopane index (Peters and Moldowan, 1991) may suggest oxic conditions, while the Pr/Ph ratio <1 and relatively high DBT content coupled with the high ratios of *Ts*/*Tm* (Moldowan et al., 1986) are suggestive of dysoxic conditions within the environment (Table 2).

5.2. Section 2

In this section, the Baghamshah formation with a thickness of 650 m consists of dark gray marls with some intercalations of highly porous brown siltstone/sandstone and wood debris (Figure 3). The decrease in HI with increasing TOC for the samples from this section (Figure 2a) may be a consequence of increasing levels of oxygenation during deposition, intensive bacterial reworking during or after the deposition of the OM, and/or increasing the contribution of terrestrial OM to the environment. However, distinguishing between the imprint of each of these processes may demand further analyses.

The gas chromatographic results of a sample from Section 2 (Figure 4) indicate a predominance of n-alkanes in the C_{15}-C_{16} range, consistent with the bacterial source of organic input (Hunt, 1996; Murray et al., 1994; Peters et al., 2005). Prevailing oxic conditions in the depositional setting may have resulted in the pronounced formation of pristane relative to phytane from the original bacterial input and a consequent increase in the pristane/phytane ratio (Didyk et al., 1978; Volkman, 1988; Volkman and Maxwell, 1986). Additional support for this assumption is provided by the GCMS data as can be seen in Figure 4.

The relatively high values for the $C_{24}Tt/C_{26}t$ in Table 2 (2.03) (Hughes and Holba, 1988), high hopane/sterane ratio (2.90) (Tissot and Welte, 1984), low values of *Ts*/*Tm* (0.41) (Moldowan et al., 1986), and a high relative abundance of lower isoprenoids over the GC profiles (Figure 4) (Albaigés et al., 1985; Brassell et al., 1986a; Lijmbach, 1975) might support the possibility of bacterial reworking. In addition, the very low TAR and very high short/long n-alkane ratios (Table 2) are signs of minor terrestrial OM contribution (Peters et al., 2005).

It is evident from the data presented in Table 2 that Section 2 has been deposited under fresh water oxic conditions. The very low Gammacerane Index (0.07) (Curiale et al., 1985; Moldowan et al., 1985) very low R_{22} (0.87) (Ten Haven et al., 1988), and the absence of bisnorhopanes (Rogers et al., 1999) all suggest low salinity conditions prevailing in this locality. In addition, relatively low *Ts*/*Tm* ratio (0.41) for the sample from this section may indicate oxic environmental conditions (Moldowan et al., 1986), in line with the low moretane/hopane ratio (0.42) (Rullkötter and Marzi, 1988) (Table 2).

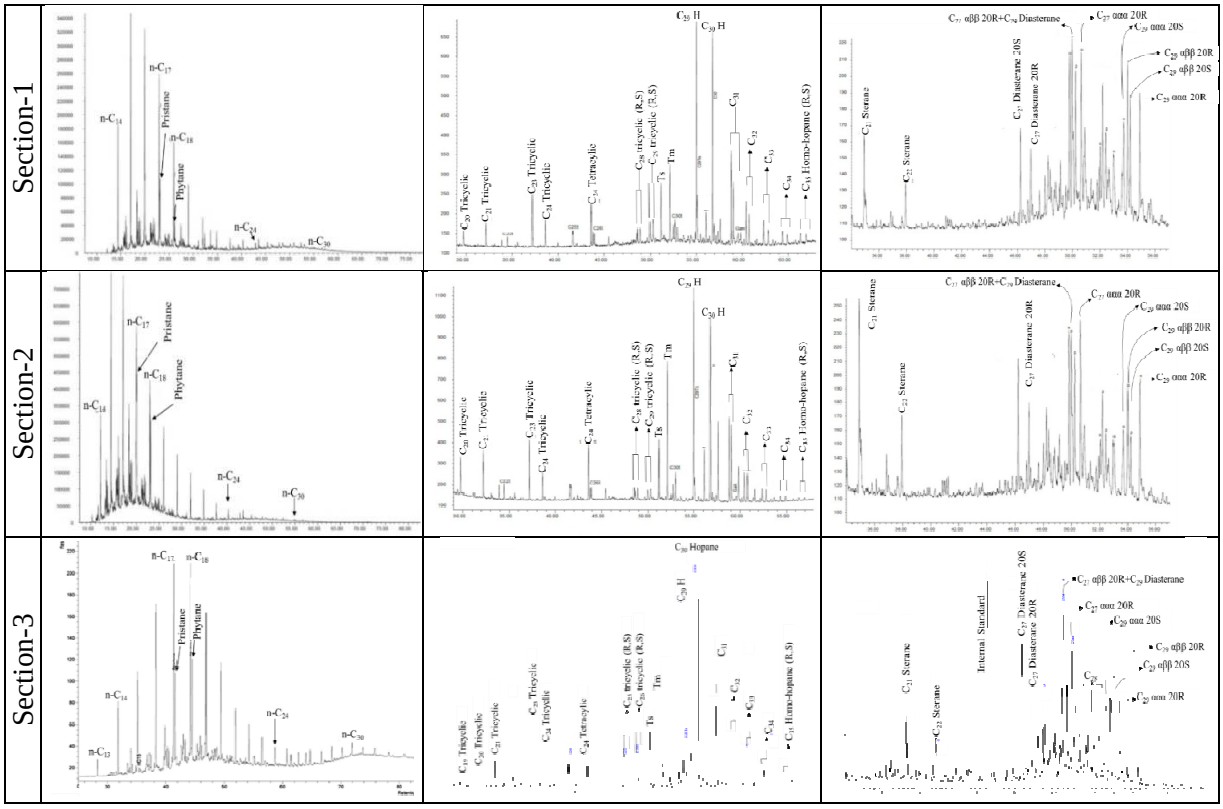

Figure 4
Total ion chromatograms (GC) and m/z 191 and 217 mass chromatograms for Sections 1-3.

5.3. Section 3

The Baghamshah formation in this section is composed of 410 m of gray shale and marl with some intercalations of fossiliferous coral limestone towards the upper parts of the section (Figure 3). The HI/TOC relationship of the samples from Section 3 is more or less similar to that of the samples from Section 2, except for the comparatively lower HI values observed for the former (Figure 2a).

The gas chromatographic results of this section are in agreement with an increase in the amount of terrestrial input into the environment. Relatively speaking, the n-alkane distribution peaks at higher homologues (n-C_{18} compared to n-C15 in Sections 1 and 2 respectively) and a small hump of UCM appears in the C_{30}-C_{35} n-alkane range (Figure 4). This is in accordance with the relatively higher TAR and lower short/long n-alkane ratios (Table 2).

Further support for the increased terrestrial contribution in this locality includes the high hopane/sterane ratio (average of 4.91) (Figure 7a) and relatively higher C_{29}/C_{27} sterane ratio (average of 0.92) (Figure 7b and Table 2). It is noteworthy that the decrease in the concentration of the C_{24} tetracyclic terpanes (lower $C_{24}Tt/C_{23}t$ ratio) is in contrast with this conclusion. However, the lower concentrations of carbonate in this section (also note very low C_{29}/C_{30} H ratio) may explain this discrepancy (Figure 6a), since higher concentrations of $C_{24}Tt$ are also reported to associate with carbonate lithology (Connan et al., 1986).

Table 2
Bulk geochemical and molecular parameters of extracts from 6 Baghamshah outcrop sections.

	Section	1	2	3		4	5		6	
	Samples No.	*T-2321*	*T-2578*	*T-731*	*T-813*	*T-2420*	*T-1961*	*T-1721*	*T-2789*	*T-2916*
GC	Pr/Ph	0.93	1.76	0.91	1.26	0.94	0.97	0.88	0.77	0.74
	CPI	0.91	1.07	1	0.98	1.01	0.79	0.86	0.95	1.02
	TAR	0.18	0.03	0.25	0.14	0.34	0.36	0.17	0.28	0.07
	R_{22}	1.23	0.87	0.96	1.00	1.08	1.11	1.28	0.96	1.10
GC-MS	S/L n-alkanes	4.32	16.33	5.13	7.22	2.40	2.00	3.67	3.57	13.70
	$C_{22}t/C_{21}t$	0.44	0.42	0.39	0.32	0.48	0.56	0.47	0.52	0.51
	$C_{24}t/C_{23}t$	0.55	0.50	0.61	0.48	0.53	0.54	0.5	0.56	0.42
	$C_{26}t/C_{25}t$	0.83	0.87	0.91	0.72	0.94	0.96	0.79	0.99	0.74
	$C_{24}Tt/C_{26}t$	1.51	2.03	0.93	1.69	2.60	1.64	1.82	1.54	2.23
	$C_{24}Tt/C_{30}H$	0.18	0.28	0.16	0.16	0.10	0.54	0.25	0.33	0.66
	$C_{23}t/C_{30}H$	0.23	0.32	0.28	0.42	0.09	0.62	0.31	0.33	0.96
	$C_{24}Tt/C_{23}t$	0.81	0.88	0.55	0.38	1.20	0.87	0.5	1.01	0.68
	C_{30} t/(Ts+Tm)	0.39	0.24	0.21	0.17	0.14	0.22	0.33	0.26	0.25
	C_{24} t/C_{26}t	1.03	1.15	1.04	2.12	1.14	1.01	1.13	0.86	1.35
	% tt	16.61	21.28	19.10	27	8.82	27.15	19.9	23.15	33.32
	% pt	55.30	58.85	55.00	55.7	78.54	42.42	51.68	52.56	41.37
	% St	28.09	19.87	25.90	17.3	12.63	30.43	28.42	24.29	25.31
	$C_{29}/C_{30}H$	0.95	0.95	0.78	0.76	0.77	1.07	0.98	0.99	0.89
	$C_{31}R/C_{30}H$	0.36	0.42	0.26	0.33	0.36	0.30	0.32	0.29	0.35
	G/H	0.11	0.07	0.03	0.03	0.05	0.10	0.13	0.11	0.16
	C_{35}/C_{34} H	0.76	0.93	0.66	0.68	0.64	1.26	0.87	1.24	1.22
	M/H	0.12	0.42	0.19	0.32	0.44	0.10	0.08	0.1	0.15
	H/St	1.97	2.90	4.07	5.75	6.72	1.36	2.11	2.51	1.96
	Ts/Tm	0.74	0.41	0.64	0.47	0.13	0.88	0.73	0.88	0.88
	22S/(22S+22R)	0.57	0.50	0.60	0.55	0.59	0.57	0.58	0.6	0.57
	C_{27}Dia/(Dia+Reg) St	0.08	0.12	0.53	0.46	0.12	0.11	0.09	0.12	0.16
	C_{29}/C_{27} St	0.59	0.70	0.92	0.92	0.81	0.38	0.52	0.39	0.53
	20S/(20S+20R)	0.47	0.39	0.48	0.39	0.50	0.50	0.49	0.53	0.44
	C_{29} αββ/(ααα+αββ)	0.52	0.44	0.53	0.47	0.44	0.55	0.53	0.56	0.54
	DBT/Phen	0.77	0.72	0.19	0.50	0.13	0.69	0.78	0.71	0.53
	S/(S+L) MAS	0.34	0.09	n.d.	0.39	0.03	0.38	0.29	0.01	0.01
Extraction	Saturate HCs (%)	47.50	39.50	21.90	60	38.50	44.50	37.5	38	41.00
	Aromatic HC (%)	30.50	24.50	50.70	10	29.50	26.50	24.5	27.5	32.50
	Polar (%)	22.00	36.00	27.40	24.9	32.00	29.00	38	34.5	26.50
	Asphaltene (%)	2.00	2.50	0.00	5.1	1.50	4.50	6.5	4	2.50

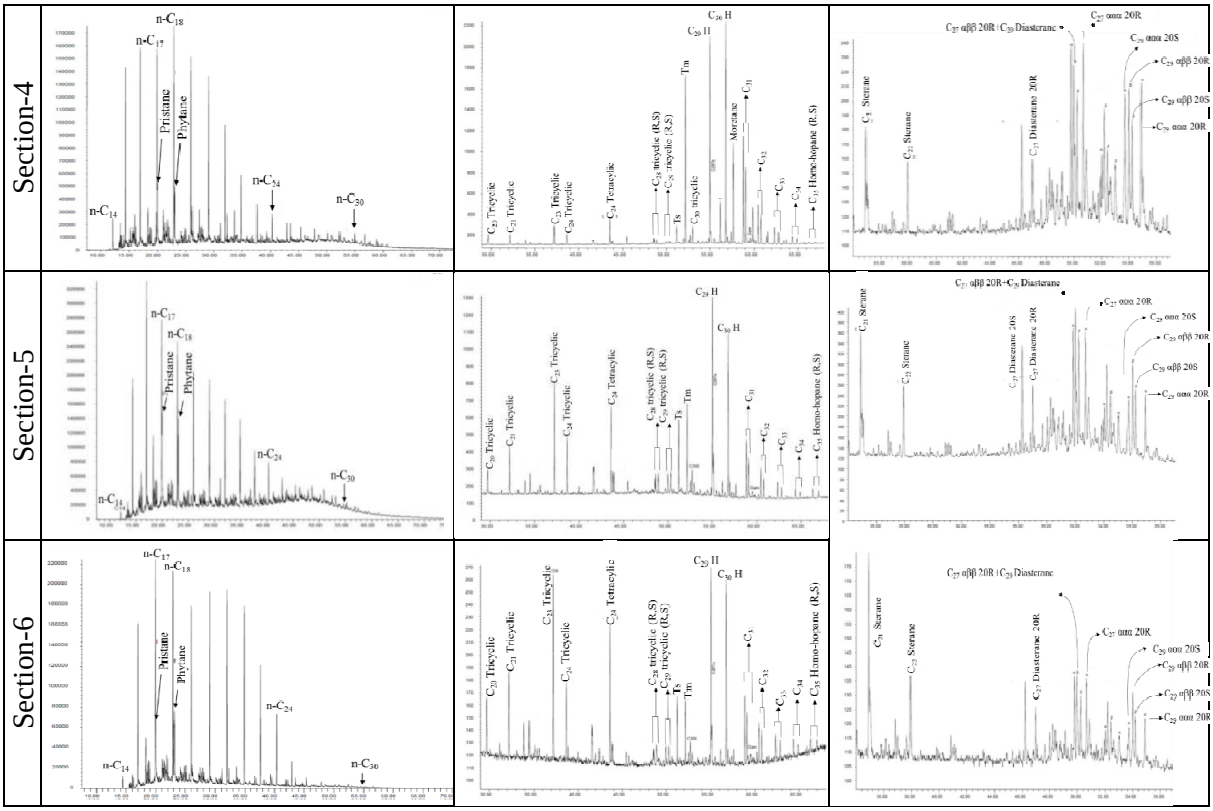

Figure 5
Total ion chromatograms (GC) and m/z 191 and 217 mass chromatograms for Sections 4-6.

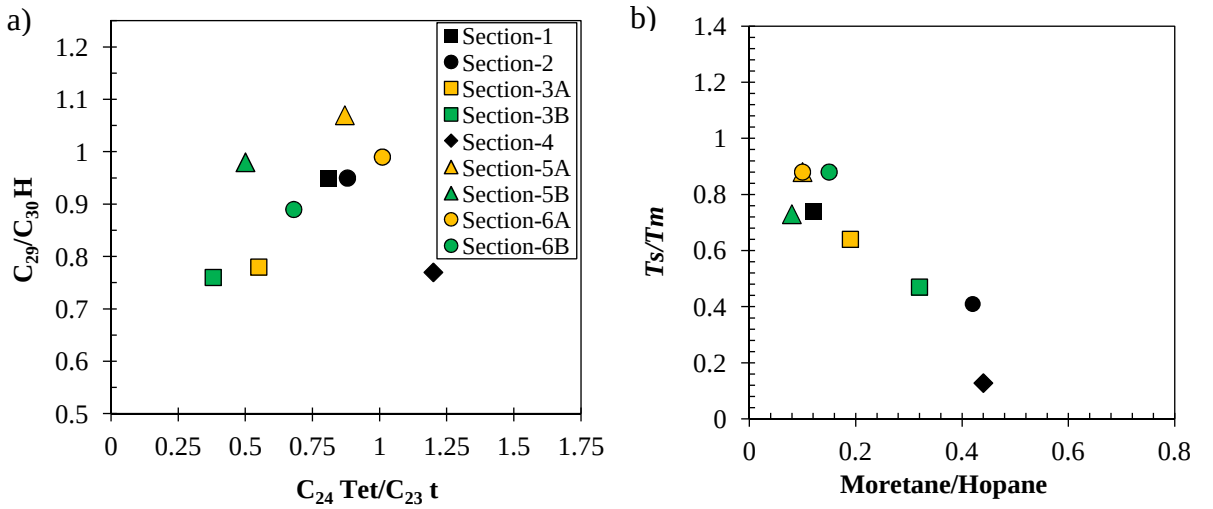

Figure 6
Plots of C_{29}/C_{30} hopane versus C_{24} tetracyclic/C_{23} tricyclic terpanes ratio (a); the higher C_{24} tetracyclic ratio for Section 4 is evidence for its terrestrial character; *Ts*/*Tm* versus moretane/hopane (b).

The decrease in the salinity of the depositional environment in this section is evident from the very low Gammacerane Index (average of 0.03) and low R_{22} values (average of 0.98). Moreover, the decrease in the C_{35}/C_{34} homohopane ratio (average of 0.67, Figure 8a), the lower moretane/hopane ratio (average of 0.26, Figure 7a), and the relatively higher concentrations of diasteranes (average C_{27} Dia/(Dia+Reg) ratio of 0.50) are in conformity with the increased levels of oxicity in the depositional environment.

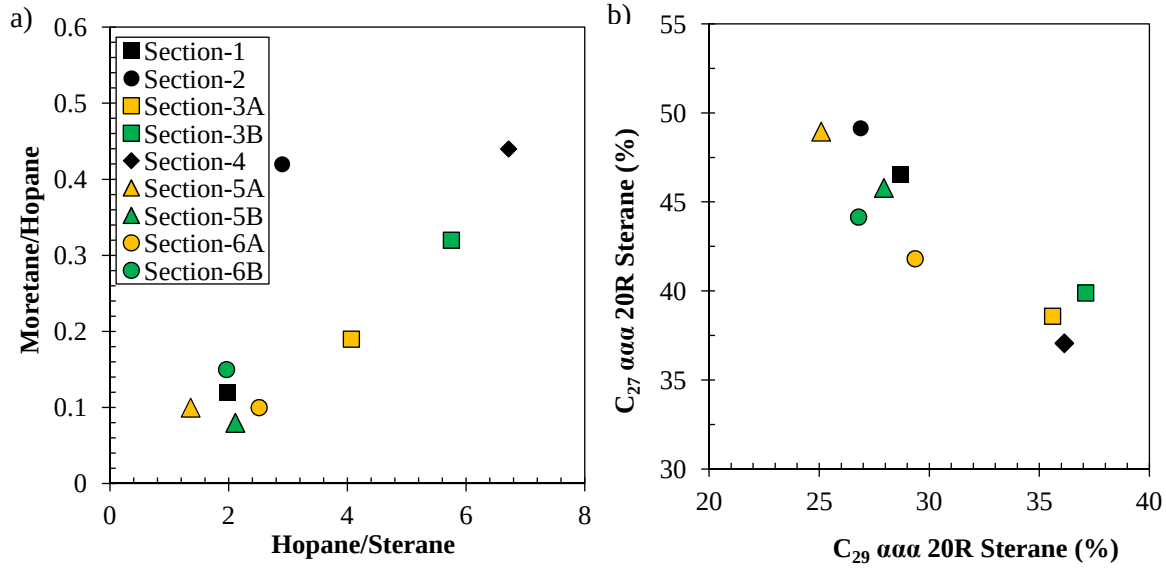

Figure 7
Plots of moretane/hopane versus hopane to sterane ratio (a) and C_{27}ααα 20R versus C_{29} ααα 20R regular sterane (b) indicating variations in the intensity of terrigenous effect in the studied sections.

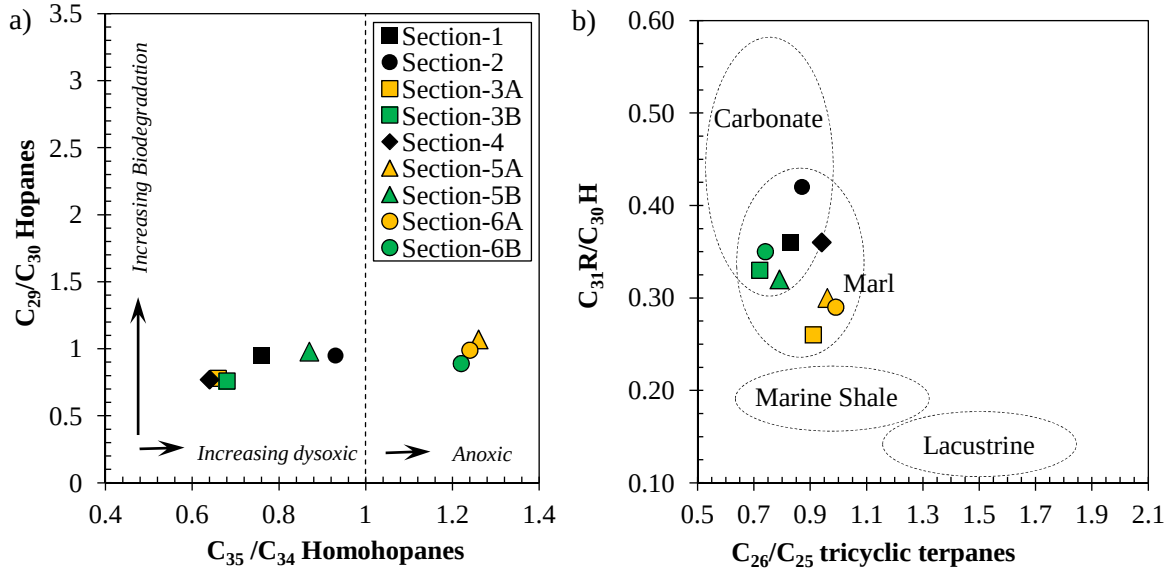

Figure 8
Plots of C_{29}/C_{30} hopane versus C_{35}/C_{34} homohopanes ratio (a), for determining oxicity of the environments and C31R/C30hopane versus C_{26}/C_{25} tricyclic terpanes ratio (b) (both diagrams after Peters et al., 2005).

5.4. Section 4

The lowest thickness of the Baghamshah formation among the studied sections belongs to Section 4, where it comprises of about 350 m of gray marls with minor silt (Figure 3). The inverse HI/TOC relationship and very low HI values (in some samples) are assumed to be a consequence of input from a secondary (more oxidized) source and/or oxidative degradation of the organic matter during deposition (Figure 2a). This conclusion is better supported by the GC profile obtained for a representative sample from this section (Figure 5) as well as by the other biomarker ratios (see below).

The apparent odd-to-even preference in the distribution of n-alkanes and the comparatively higher concentration of HMW n-alkanes are indicative of strong terrestrial (Hunt, 1996) and/or fresh water algal effect in this section (McKirdy et al., 1986). However, the very low *Ts*/*Tm* (0.13) (Moldowan et al., 1986) and the relatively high moretane/hopane ratio (0.44) are in line with higher terrestrial input (Figure 6b). Of particular interest is the concentration of C_{24} tetracyclic terpanes that reaches the highest value in this section (Table 2). This, coupled with the lowest C_{29}/C_{30} hopane ratio, suggests a strong terrestrial effect on this section (Figure 6a) (Connan et al., 1986; Mello et al., 1988). The hopane/sterane ratio has its highest value (6.72) (Figure 7a) in this section, which is indicative of predominantly terrigenous OM (Peters et al., 2005; Tissot and Welte, 1984) deposited under less marine conditions (Moldowan et al., 1985).

The very low Gammacerane Index (0.05) and the low value for the R_{22} (1.08) are indications of OM deposited under a fresh-water environment with lower salinity relative to the other sections (Table 2). Moreover, the concentration of the tricyclic terpanes reaches its lowest amount in this section, which is consistent with the lower salinity in the depositional environment (Huang, 2000).

According to the published literature, the lower salinity coincides with the elevated oxicity within the paleoenvironment of this section. The evidence for this conclusion comes from the very low values of DBT/Phen (0.13) (Hughes, 1984; Hughes et al., 1995), very low ratio of C_{35}/C_{34} homohopane (0.64, Figure 8a), the very low *Ts*/*Tm* ratio (0.13), and the very low value for the Gammacerane Index (0.05) (Table 2). Moldowan et al. (1986) suggested that ratios of the short/(short+long) MAS tend to decrease with increasing the anoxicity of the environment; however, the very low value (0.03) for this ratio is not in agreement with the lower C_{35}/C_{34} homohopane ratio. The reason for this discrepancy is currently not well understood and further research is required for explaining this observation.

5.5. Section 5

With a thickness of about 1000 m, the Baghamshah formation is mainly composed of dark, occasionally pencil, calcareous shales with several thin intercalations of siltstone (Figure 3). Compared to the other sections, an abrupt increase in the thickness of the formation is evident.

Among the gas chromatograms of the samples analyzed from this section, the n-alkane homologues distribution maximizes at n-C_{16} and the HMW homologues are relatively more abundant (Figure 5). In addition, the distribution of n-alkanes indicates a strong even-over-odd preference in the n-C_{16} to n-C_{24} range. The predominance of even-numbered n-alkanes is in agreement with the highly reducing anoxic environment and/or carbonate/evaporate lithology of the source rock (Connan et al., 1986). This is also indicated by the abnormally high concentrations of LMW steranes over the m/z 217 mass chromatograms (Figure 5). These compounds are highly specific for the hypersaline depositional conditions (Ten Haven et al., 1985) or marine carbonate environments (Mello et al., 1988).

Compared to the other sections, a major contribution from terrestrial source is less likely in this section. Various biomarker parameters such as very low C_{29}/C_{27} sterane ratio (average of 0.45, Figure 7b), relatively low TAR (average 0.26), lower hopane/sterane ratio compared to the other sections (average 1.73, Figure 7a), very low moretane/hopane ratio (average 0.09, Figure 7a), and relatively high *Ts*/*Tm* ratio (average 0.81, Figure 6b) are consistent with the reduced terrestrial input in this section. It is noteworthy that the higher concentration of C_{24} tetracyclic terpanes (average $C_{24}Tt/C_{23}t$ ratio of 0.69) can be a reflection of the mainly carbonate lithology of the studied formation (Palacas, 1983), which is also supported by the relatively higher C_{29}/C_{30} hopane ratio (average of 1.03, Figure

6a) (Peters et al., 2005; Zumberge, 1987) and the even-over-odd predominance of n-alkanes mentioned previously.

The relative increase in the salinity of the depositional environment in this section is indicated by the comparatively high ratios of R_{22} (average 1.19), higher Gammacerane Index (average 0.12), and higher DBT/Phen ratio (average 0.73) relative to the other sections (Table 2).

Moreover, the higher C_{35}/C_{34} homohopane ratio (average 1.07, Figure 8a), the very low ratios of C_{27}Dia/(Dia+Reg) sterane (average 0.1), and the relatively high DBT/Phen ratio are indications of the less oxic depositional conditions in this section (Table 2). It is noteworthy that the short/ (short+long) MAS ratio (average 0.33) is relatively higher than what is expected for this section (Table 2).

5.6. Section 6

The Baghamshah formation in this section comprises of 800 m of shale and argillaceous limestone with widespread inter-layers of carbonate and siltstone intercalations (Figure 3).

The gas chromatographic results of the samples from this section are in conformity with the predominance of LMW n-alkanes, suggesting the very small, if any, contribution of terrestrial OM (Figure 5). This is further supported by the very low TAR (average 0.17) and relatively low Pr/Ph ratio (average 0.75). Additional support for the low terrestrial input in this section comes from GCMS data (Table 2). Generally, the noticeably low C_{29}/C_{27} sterane ratio (average of 0.46, Figure 7b), very low moretane/hopane ratios (average 0.13, Figure 7a), relatively higher *Ts*/*Tm* ratio (average 0.88, Figure 6b), and a higher relative concentration of tricyclic terpanes (average $C_{23}t/C_{30}H$ ratio of 0.65, Table 2) are in agreement with the very low terrestrial impact. However, the possibility of a secondary bacterial/terrestrial source cannot be ruled out because the hopane/sterane ratio is greater than unity.

The relatively high salinity of the depositional environment in this section is deduced from the higher relative Gammacerane Indices (average 0.14) and relatively higher R_{22} (average 1.03) (Table 2). Moreover, the high C_{35}/C_{34} homohopane ratios (average 1.23, Figure 8a) coupled with the very low short/(short+long) MAS ratios (average 0.01), low Pr/Ph ratios (average 0.75), and high *Ts*/*Tm* (average 0.88) are in accordance with the less oxic conditions for the organic matter deposited in this section.

5.7. Paleoenvironmental implications

Variations in the composition of the solvent extractable OM from the Middle Jurassic Marls of the Baghamshah marls provide valuable findings about their prevailing paleodepositional conditions. Generally, the studied formation is comprised of marls (Figure 8b) deposited in marine conditions as suggested by the significantly high short-/long-chain n-alkane ratios for all the studied sections (2.0-16.33), the very low TAR values (0.07-0.36), and the generally low CPI values (0.79-1.07) (Peters et al., 2005) (Table 2). This is well in accordance with the stratigraphic findings of Wilmsen et al. (2010), who suggested an open-marine setting for Baghamshah formation. The generally low values of Gammacerane Index (0.03-0.16) suggest low-salinity conditions with relatively higher levels of oxicity for the studied formation. Finally, the hopane/sterane ratios >1, the *Ts*/*Tm* ratios <1, and moretane/hopane ratios <0.5 for all the studied sections are consistent with the bacterial OM as a major contributor to the environment of the studied marls; however, ubiquitous terrigenous contributions with some variations among the studied sections have also been suggested based on other ratios.

According to the results presented, variations in the original organic input, salinity, and redox conditions across the studied sections could be monitored regionally. Comparing various biomarker ratios provides an appraisal of the relative intensity of terrestrial effect, salinity, and oxicity in each section. A gradual increase in the terrestrial effect from Section 1 towards Section 4, where it reaches the maximum value, and then an abrupt decrease in Sections 5 and 6 is seen.

Variations in salinity of the depositional environment are also evident. There is a continuous decrease in salinity from Section 1 towards Section 4, followed by an abrupt increase in Sections 5 and 6.

Generally speaking, the oxicity of the Baghamshah depositional environment is suggested to be relatively high. However, the level of oxicity varies in accordance with the salinity among the studied sections. In other words, the oxicity increases from Section 1 to Section 4, reaching the highest value in Section 4, while it drops to orders of magnitude lower values in Sections 5 and 6.

The reconstruction presented in this paper honors the observed trend of the variations in biomarker ratios. Notwithstanding the small number of the studied sections (the possibility that the total number of samples analyzed from each section may not be representative of the entire formation), it summarizes the latest organic geochemical data on the Middle Jurassic of the area. According to the results obtained, the decrease in the salinity and the increase in both oxicity and terrestrial input are in agreement with a decrease in the depositional depth towards Section 4. Our conclusion is supported with a continuous decrease in the thickness of the Baghamshah formation towards central areas (note thickness variation among Sections 1 through 4). Assuming the main clastic input from the adjacent Yazd Block, also suggested by Wilmsen et al. (2009), seems to be more conformable with the existing scenario. Section-4 occupies a more proximal position to the northern corner of the Yazd Block and is thought to receive the highest fluvial discharge (which is in agreement with its higher terrestrial input, lower salinity, and higher oxicity) with the other sections receiving lower contribution as we move southward (Figure 9).

The sudden shift in salinity with a parallel fall in the oxicity and terrestrial input for Sections 5 and 6 suggest an abrupt deepening of this part of the Baghamshah basin. We presume a fault zone across the northern and southern Shotori Mountains as schematically illustrated by a dashed line on Figure 9.

The likelihood of this fault scenario is additionally supported by evidence coming from geological maps of the area. It is clearly noted that the older sediments of Carboniferous and Permian age expose on the surface (due to the activity of some local thrust faults) within the southern Shotori Mountains (see Figure 9). In contrast, there are no indications of these Carboniferous/Permian outcrops in the northern area meaning that the aforementioned thrust faults have been truncated at depth by our proposed fault line. No other scenarios can adequately explain the current observations and answer the following two questions:

(1) Why do the majority of geochemical parameters in Sections 5 and 6 (Figures 1 and 10) display conspicuously deeper, less-oxic character?

(2) What is the reason for the general absence of Carboniferous/Permian outcrops in the same location (vicinity of sections 5 and 6)?

Nevertheless, we think that verifying the fault plane and its activity falls beyond the scope of the current paper and may require additional field and structural information.

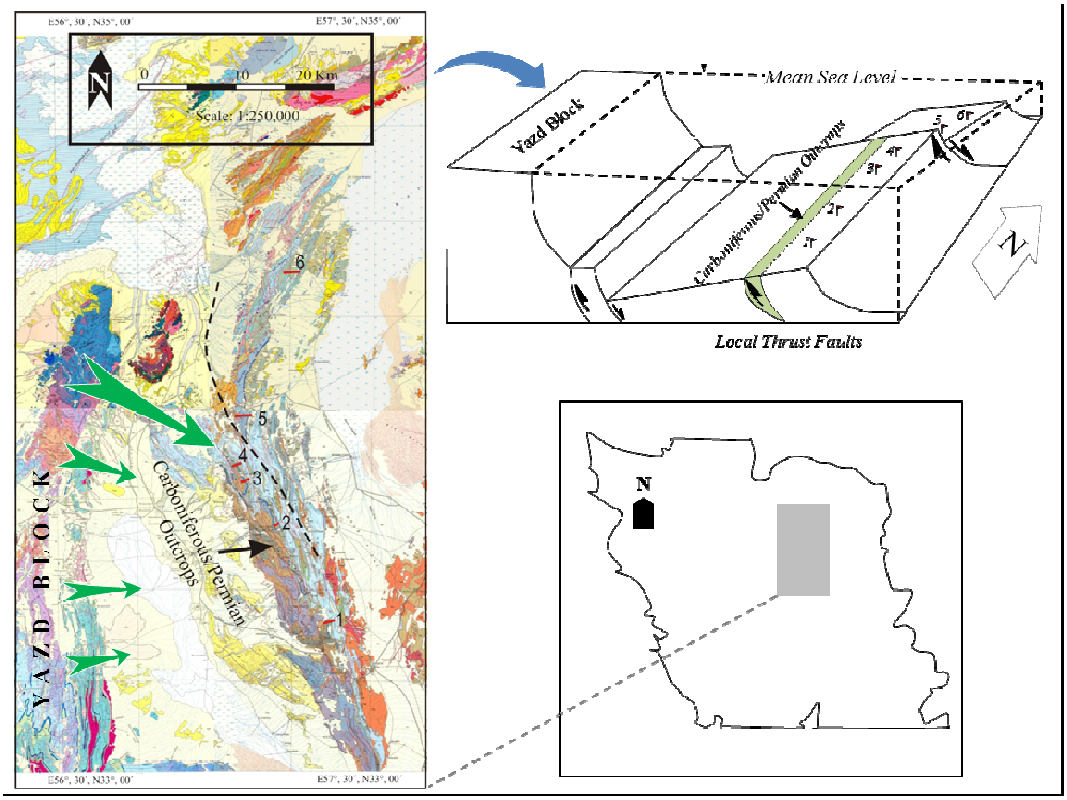

Figure 9
Predominant flow regimes (green arrows), Carboniferous-Permian outcrops, a hypothetical fault line (dashed line) and Paleogeomorphologic model of Middle Jurassic.

6. Conclusions

Samples from the Middle Jurassic Baghamshah formation were collected from six outcrop sections along the Shotori swell to infer about its paleodepositional conditions by looking at the organic geochemical clues contained within the indigenous OM. According to the biomarker results, the northern and southern parts of the Shotori swell have experienced different evolutionary stages in the past. Within the southern Shotori Mountains, an increase in the level of oxicity of Baghamshah basin northward coupled with the decrease in the salinity and an increase in the terrestrial OM input in the same direction suggest a decrease in the depth of the basin to the north. The proximity of the Yazd Block to the northernmost parts of the southern Shotori Mountains may explain these observations. Compared with the southern Shotori Mountains, the depth of the Baghamshah basin across the northern Shotori Mountain is expected to be higher as suggested by various parameters and stratigraphic observations. Based on these results, a paleoenvironmental model is proposed for the studied area with a fault separating the northern and southern Shotori Mountains. A probable orientation for future studies can be establishing a detailed stratigraphic correlation among the sections. This would enable piloting enhanced sampling strategies (where we could pick samples from the same sedimentary cycles/facies of the Baghamshah formation within all the studied sections), and thereby increasing the resolution of interpretations.

8. Acknowledgments

The authors would like to extend their acknowledgements to the exploration directorate of the National Iranian Oil Company (NIOC) for providing the data and for the financial support of the

analysis. In addition, the Petroleum Geology and Geochemistry Research Centre (PGGRC) of S. Chamran University of Ahwaz is warmly acknowledged for performing some of the analyses. Special thanks are also due to Prof. Seyed-Emami (University of Tehran) for critical comments about the stratigraphy of the studied area. Finally, the anonymous reviewers of an earlier version of this manuscript are sincerely acknowledged for their constructive comments, which greatly enhanced the quality of the work.

Nomenclature

TOC	: Total organic carbon
SOM	: Sedimentary organic matter
Pr/Ph	: Pristane/phytane ratio
CPI	: Carbon preference index
TAR	: Terrigenous to aquatic ratio $(C_{27}+C_{29}+C_{31})/(C_{15}+C_{17}+C_{19})$
R_{22}	: $2*(n\text{-}C_{22})/ (n\text{-}C_{21}+n\text{-}C_{23})$
S/L n-alkanes	: Short/long n-alkanes= $(C_{17}+C_{18}+C_{19})/(C_{27}+C_{28}+C_{29})$
$C_{22}t/C_{21}t$	: C_{22} tricyclic terpane/C_{21} tricyclic terpane ratio
$C_{24}Tt/C_{26}t$	: C_{24} tetracyclic terpane/C_{26} tricyclic terpane ratio
% tt	: Percent tricyclic terpanes
% pt	: Percent pentacyclic terpanes
% St	: Percent pentacyclic terpanes
G/H	: Percent steranes
C_{35}/C_{34} H	: C_{35} Homohopane (20S+20R)/C_{34} homohopane (20S+20R) ratio
M/H	: Moretane/hopane ratio
H/St	: Hopane/sterane ratio
Ts/*Tm*	: 22,29,30,18a(H)-neohopane (*Ts*)/ 22,29,30,17a-Trisnorhopane (*Tm*)
22S/(22S+22R)	: C_{31} homohopane 22S/(22S+22R)
C_{29}/C_{27} St	: C_{29}/C_{27} ααα 20R sterane ratio
20S/ (20S+20R)	: C_{29} regular sterane 20S/(20S+20R) ratio
C_{29} αββ/(ααα+αββ)	: C_{29} regular sterane αββ/(ααα+αββ) ratio
DBT/Phen	: Dibenzothiophene/phenanthrene ratio
S/(S+L) MAS	: Short/(short+long) monoaromatic steroids ratio = (21+22)MAS/(21+22+27+28+29)MAS]

References

Albaigés, J., Borbon, J., and Walker II, W., Petroleum Isoprenoid Hydrocarbons Derived from Catagenetic Degradation of Archaebacterial Lipids, Organic Geochemistry, Vol. 8, No. 4, p. 293-297, 1985.

Alizadeh, B., Alipour, M., Hosseini, S. H., and A, J. A., Paleoenvironmental Rreconstruction using Biological Markers for the Upper Triassic–Middle Jurassic Sedimentary Succession in Tabas Basin, Central Iran, Organic Geochemistry, Vol. 42, p. 431-437, 2011.

Clayton, J. and King, J., Effects of Weathering on Biological Marker and Aromatic Hydrocarbon Composition of Organic Matter in Phosphoria Shale Outcrop, Geochimica et Cosmochimica Acta, Vol. 51, No. 8, p. 2153-2157, 1987.

Connan, J., Bouroullec, J., Dessort, D., and Albrecht, P. The Microbial Input in Carbonate-anhydrite Facies of a Sabkha Palaeoenvironment from Guatemala: A Molecular Approach, Organic Geochemistry, Vol. 10, No. 1-3, p. 29-50, 1986.

Curiale, J. A., Cameron, D., and Davis, D. V., Biological Marker Distribution and Significance in Oils and Rocks of the Monterey Formation, California. Geochimica et Cosmochimica Acta, Vol. 49, p. 271-288, 1985.

Dembicki Jr, H., Three Common Source Rock Evaluation Errors Made by Geologists during Prospect or Play Appraisals, AAPG bulletin, Vol. 93, No. 3, p. 341-356, 2009.

Didyk, B., Simoneit, B., Brassell, S. t., and Eglinton, G., Organic Geochemical Indicators of Palaeoenvironmental Conditions of Sedimentation, Nature, Vol. 272, p. 216-222, 1978.

Espitalié, J., Laporte, J. L., Madec, M., Marquis, F., Leplat, P., Paulet, J., and Boutefeu, A. Méthode Rapide de Caractérisation des Roches Mètres, de Leur Potentiel Pétrolier et de Leur Degré D'évolution, Oil & Gas Science and Technology, Vol. 32, No. 1, p. 23-42, 1977.

Fürsich, F. T., Wilmsen, M., Seyed-Emami, K., and Majidifard, M. R., Evidence of Synsedimentary Tectonics in the Northern Tabas Block, East-central Iran: the Callovian (Middle Jurassic) Sikhor Formation, Facies, Vol. 48, No. 1, p. 151-170, 2003.

Goossens, H., De Leeuw, J., Schenck, P., and Brassell, S., Tocopherols as Likely Precursors of Pristane in Ancient Sediments and Crude Oils, Nature, Vol. 312, p. 440-442, 1984.

Huang, H., The Nature and Origin of Petroleum in the Chaiwopu Sub-basin (Junggar basin), NW China, Journal of Petroleum Geology, Vol. 23, p. 193-220, 2000.

Hughes, W. B., Use of Thiophenic Organosulfur Compounds in Characterizing Crude Oils Derived from Carbonate versus Siliciclastic Sources, 1984.

Hughes, W. B., and Holba, A. G., Relationship between Crude Oil Quality and Biomarker Patterns, Organic Geochemistry, Vol. 13, No. 15-30, 1988.

Hughes, W. B., Holba, A. G., and Dzou, L. I., The Ratios of Dibenzothiophene to Phenanthrene and Pristane to Phytane as Indicators of Depositional Environment and Lithology of Petroleum Source Rocks, Geochimica et Cosmochimica Acta, Vol. 59, p. 3581-3598, 1995.

Hunt, M., Petroleum Geochemistry and Geology, Freeman and Company, NewYork, 1996, 743 pages.

Isaksen, G. and Bohacs, K., Geological Controls of Source Rock Geochemistry through Relative Sea Level; Triassic, Barents Sea, In: Petroleum Source Rocks (Katz BJ ed), p. 25-50, Springer Berlin Heidelberg, 1995.

Katz, B. J., Limitations of 'Rock-Eval'Pyrolysis for Typing Organic Matter, Organic Geochemistry, Vol. 4, p. 195-199, 1983.

Leythaeuser, D., Effects of Weathering on Organic Matter in Shales, Geochimica et Cosmochimica Acta, Vol. 37, p. 113-120, 1973.

Lijmbach, W., On the Origin of Petroleum. 9th World Petroleum Congress, Vol. 2, p. 357-369, Tokyo, Japan, 1975.

Lo, H. and Cardott, B., Detection of Natural Weathering of Upper McAlester Coal and Woodford Shale, Oklahoma, USA, Organic Geochemistry, Vol. 22, p. 73-83, 1995.

Marynowski, L., Kurkiewicz, S., Rakociński, M., and Simoneit, B. R., Effects of Weathering on Organic Matter: I. Changes in Molecular Composition of Extractable Organic Compounds Caused by Paleoweathering of a Lower Carboniferous (Tournaisian) Marine Black Shale, Chemical Geology, Vol. 285, No. 1-4, p. 144-156, 2011.

Mello, M., Gaglianone, P., Brassell, S., and Maxwell, J., Geochemical and Biological Marker Assessment of Depositional Environments using Brazilian Offshore Oils, Marine and Petroleum Geology, Vol. 5, p. 205-223, 1988.

Moldowan, J. M., Seifert, W. K., and Gallegos, E. J. Relationship between Petroleum Composition and Depositional Environment of Petroleum Source Rocks, AAPG Bulletin, Vol. 69, p. 1255-

1268, 1985.

Moldowan, J. M., Sundararaman, P., and Schoell, M., Sensitivity of Biomarker Properties to Depositional Environment and/or Source Input in the Lower Toarcian of SW-Germany. Organic Geochemistry, Vol. 10, p. 915-926, 1986.

Murray, A. P., Summons, R. E., Boreham, C. J., and Dowling, L. M., Biomarker and< i> n</i>-Alkane Isotope Profiles for Tertiary Oils: Relationship to Source Rock Depositional Setting, Organic Geochemistry, Vol. 22, p. 521-IN526, 1994.

Ortiz, J. E., Moreno, L., Torres, T., Vegas, J., Ruiz-Zapata, B., García-Cortés, Á., Galán, L., and Pérez-González, A., A 220 ka Palaeoenvironmental Reconstruction of the Fuentillejo Maar Lake Record (Central Spain) using Biomarker Analysis, Organic Geochemistry, Vol. 55, p. 85-97, 2013.

Palacas, J., Carbonate Rocks as Sources of Petroleum: Geological and Chemical Characteristics and Oil-source Correlations, 11th World Petroleum Congress, Vol. 2, p. 31-43, London, UK, 1983.

Peters, K. and Moldowan, J., Effects of Source, Thermal Maturity, and Biodegradation on the Distribution and Isomerization of Homohopanes in Petroleum, Organic Geochemistry, Vol. 17, p. 47-61, 1991.

Peters, K. E., Walters, C. C., and Moldowan, J. M., The Biomarker Guide: Biomarkers and Isotopes in the Environment and Human History, Cambridge University Press, 2005.

Rodrigues, R., Trindade, L. A., Cardoso, J. N., and de Aquino Neto, F. R., Biomarker Stratigraphy of the lower Cretaceous of Espírito Santo Basin, Brazil. Organic Geochemistry, Vol. 13, 707-714, 1988.

Rogers, K. M., Collen, J. D., Johnston, J. H., and Elgar, N. E., A Geochemical Appraisal of Oil Seeps from the East Coast Basin, New Zealand. Organic Geochemistry, Vol. 30, p. 593-605, 1999.

Rullkötter, J. and Marzi, R. Natural and Artificial Maturation of Biological Markers in a Toarcian Shale from Northern Germany, Organic Geochemistry, Vol. 13, p. 639-645, 1988.

Seifert, W. K. and Moldowan, J. M. Paleoreconstruction by Biological Markers, Geochimica et Cosmochimica Acta, Vol. 45, p. 83-794, 1981.

Stöcklin, J., Eftekhar-Nezhad, J., and Hushmand-Zadeh, A., Geology of the Shotori Range (Tabas Area, East Iran), Geological Survey of Iran, No. 3, 1965.

Ten Haven, H., De Leeuw, J., Damsté, J. S., Schenck, P., Palmer, S., and Zumberge, J., Application of Biological Markers in the Recognition of Palaeohypersaline Environments, Geological Society, London, Special Publications, Vol. 40, p. 123-130, 1988.

Ten Haven, H., De Leeuw, J., and Schenck, P., Organic Geochemical Studies of a Messinian Evaporitic Basin, Northern Apennines (Italy) I: Hydrocarbon Biological Markers for a Hypersaline Environment, Geochimica et Cosmochimica Acta, Vol. 49, p. 2181-2191, 1985.

Tissot, B. P. and Welte, D. H., Petroleum Formation and Occurrence: A New Approach to Oil and Gas Exploration, 1984.

Volkman, J., Biological Marker Compounds as Indicators of the Depositional Environments of Petroleum Source Rocks, Geological Society, London, Special Publications, Vol. 40, p. 103-122, 1988.

Volkman, J. K. and Maxwell, J. R. Acyclic Isoprenoids as Biological Markers, Methods in Geochemistry and Geophysics, Vol. 24, p. 1-42, 1986.

Wilmsen, M., Fürsich, F. T., Seyed-Emami, K., and Majidifard, M. R. An Overview of the Stratigraphy and Facies Development of the Jurassic System on the Tabas Block, East-central Iran, Geological Society, London, Special Publications, Vol. 312, p. 323-343, 2009.

Wilmsen, M., Fürsich, F. T., Seyed-Emami, K., Majidifard, M. R., and Zamani-Pedram, M., Facies Analysis of a Large-scale Jurassic Shelf-lagoon: the Kamar-e-Mehdi Formation of East-Central Iran, Facies, Vol. 56, p. 59-87, 2010.

Zumberge, J. E., Source Rocks of the La Luna Formation (Upper Cretaceous) in the Middle Magdalena Valley, Colombia, American Association of Petroleum Geologists, Vol. 18, p. 127-133, 1984.

Zumberge, J. E., Prediction of Source Rock Characteristics Based on Terpane Biomarkers in Crude Oils: A Multivariate Statistical Approach, Geochimica et Cosmochimica Acta, Vol. 51, p. 1625-1637, 1987.